Date December 2006
Author Naaijen, P., V. Koster and R.P. Dallinga
Address Delft University of Technology
Ship Hydromechanics Laboratory
Mekelweg 2, 26282 CD Delft

TUDelft

Delft University of Technology

On the power savings by an auxiliary kite Propulsion system

by

Naaijen, P., V. Koster and R.P. Dallinga

Report No. 1502-P 2006

Publication: International Shipbuilding Progress, Volume 53, Number 4, 2006, ISSN 0020-868X

International Shipbuilding Progress

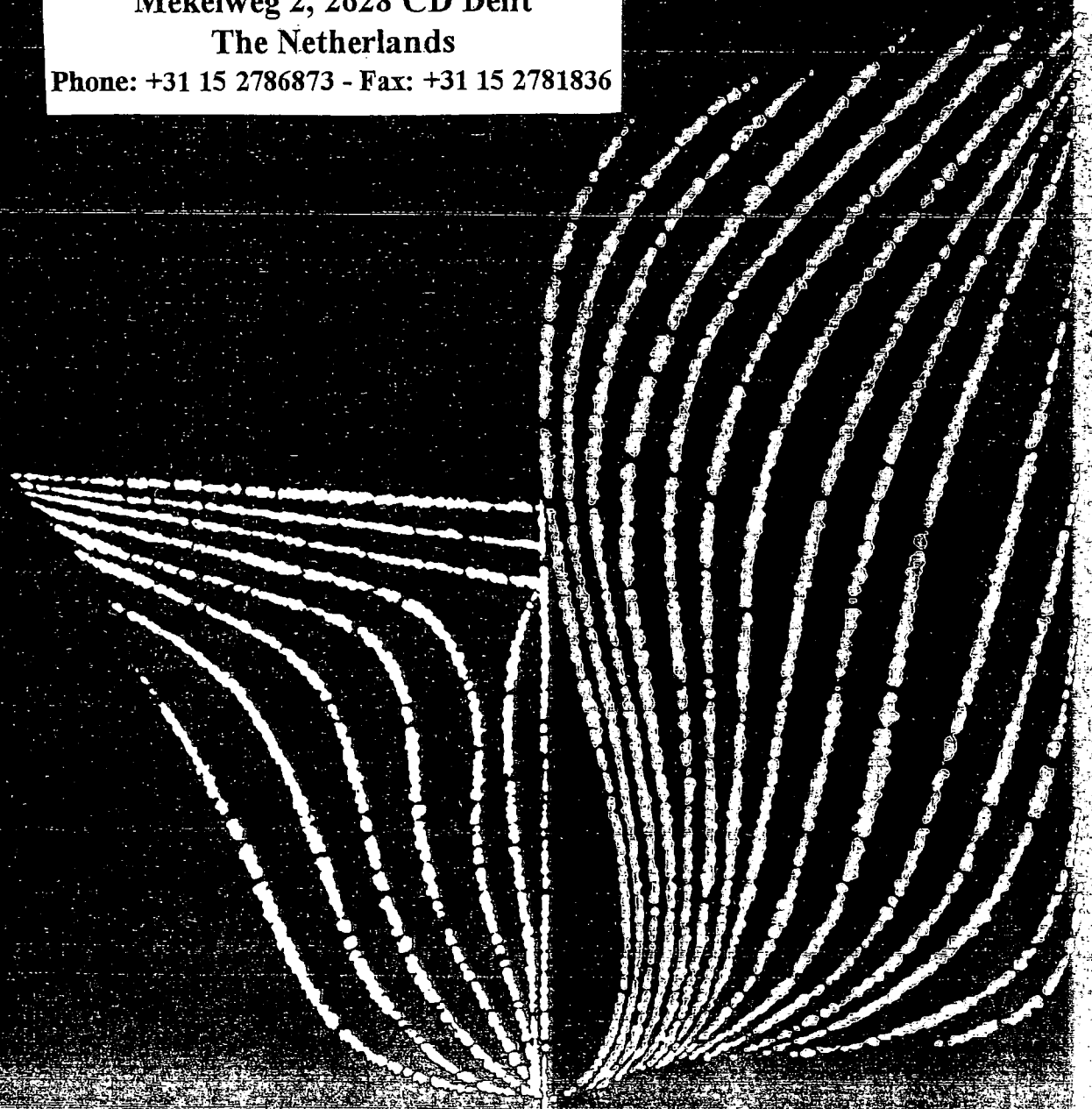

LAST NUMBER OF THIS VOLUME

IOS PRESS

ISSN 0020-868X

INTERNATIONAL SHIPBUILDING PROGRESS
Marine Technology Quarterly
Volume 53, Number 4, 2006

Contents

TU Delft
Delft University of Technology

Delft University Press is an imprint of IOS Press

International Shipbuilding Progress

Marine Technology Quarterly

Aims and scope

The journal *International Shipbuilding Progress* was founded in 1954 and is published quarterly. From 2000 the journal has also been published electronically. Publications submitted to *International Shipbuilding Progress* should describe scientific work of high international standards, advancing subjects related to the field of Marine Technology, such as: conceptual design; structural design; hydromechanics and dynamics; maritime engineering; production of all types of ships; production of all other objects intended for marine use; shipping science and all directly related subjects; offshore engineering in relation to the marine environment; ocean engineering subjects in relation to the marine environment. The contents may be of a pure scientific or of an applied scientific nature dealing with new developments and feasibility aspects.

Printed in The Netherlands

0020-868X/06/$17.00

International Shipbuilding Progress 53 (2006) 253
IOS Press

Editorial

Dear readers of *International Shipbuilding Progress*,

For those of you who do not know me yet, let me introduce myself: I am Rene Huijsmans, professor at the Ship Hydromechanics and Structures section at the Delft University of Technology. The current Editor, Jo Pinkster, is retiring as from 1 November 2006; he will step down and I will take over his position as Editor-in-Chief of the journal. I would like to thank him for his contribution to the journal.

Scope of the ISP Journal

Throughout the years, the ISP journal has gained a strong hydro mechanical and structural character. However, in the current scope of the journal, shipbuilding and design are also mentioned. Readers working in the area of ship design and ship building are also encouraged to submit manuscripts for publication in the journal.

Rene Huijsmans

Editor-in-Chief

Head Section Ship Hydromechanics and Structures
Technical University Delft
Delft, The Netherlands

International Shipbuilding Progress 53 (2006) 255–279
IOS Press

On the power savings by an auxiliary kite propulsion system

P. Naaijen [a,*], V. Koster [a] and R.P. Dallinga [b]
[a] *Delft University of Technology, The Netherlands*
[b] *MARIN, Wageningen, The Netherlands*

A performance study of auxiliary wind propulsion for commercial ships by means of a traction kite is presented. It is not focusing on practical design aspects of such a system and therefore not concluding on practical feasibility, rather it gives an indication of the amount of fuel saving in various environmental conditions assumed that the system is working practically.

An estimate is presented of the delivered traction force of a kite. Depending on the apparent wind direction and wind speed, this kite force will cause a drift angle of the ship, resulting in additional resistance. This effect is taken into account by simultaneously solving the force balance in longitudinal and lateral direction and the yaw balance.

Finally, in order to calculate the effect of auxiliary kite propulsion on the fuel consumption at constant ship speed, the performance in off-design conditions of the existing propulsion system is considered.

Results of a case study are presented showing the relative fuel saving as a function of wind speed and wind direction relative to the sailing direction.

1. Introduction

These days, renewed interest in sustainable energy solutions for transportation results in interesting concepts. One of these concepts is wind propulsion for commercial ships by means of a traction kite which is being worked on by various parties in industry.

The present study attempts to assess the benefits of this system. Design issues or operational aspects are not addressed: the theoretical question of how much fuel can be saved by means of auxiliary kite propulsion in various environmental conditions is answered, assumed that the system is functioning as it should.

High performance (high lift to drag ratio) kites similar to the ones used in sports like kite surfing and kite buggying are considered. Attached to a single tow line via a steering gondola, these kites can be actively controlled in order to create high flying speeds resulting in high traction force. Figure 1 depicts such a kite-ship system.

Compared to more conventional wind propulsion by sails, there are some benefits involved with applying kites:

*Corresponding author. E-mail: P.Naaijen@wbmt.tudelft.nl.

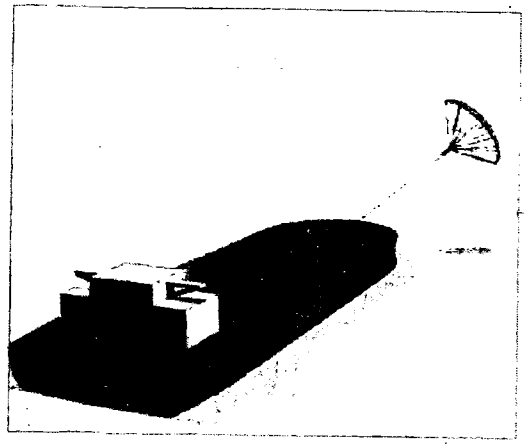

Fig. 1. Ship with kite.

- a kite can be actively controlled in order to create its own flying speed thus increasing its apparent wind speed and the traction force: more traction power can be created with less 'sail' area this way;
- due to the fact that a kite can fly at higher altitudes it is exposed to higher wind speed;
- due to the low attachment point of the tow line the roll heeling moment is considerably smaller;
- there are no masts taking deck space.

A way to estimate the kite traction force is described. The effect of the towing force by the kite on both the hull hydromechanics and the existing propulsion installation is discussed and modeled in a performance prediction program (PPP). Results in terms of relative fuel saving following from a case study are presented.

2. Kite performance

2.1. Introduction

A kite can be considered as a wing surface which enables the application of existing aerodynamic concepts: the resulting force acting on a kite is determined by calculating lift and drag on a 3D wing surface being governed by relative wind speed and angle of attack. The main assumption for the model is instantaneous equilibrium between the direction of the tow line and the direction of the resultant aerodynamic force on the kite. For a kite, this equilibrium is depending on its position in space which will be described using the so-called flight envelope (FE). The apparent wind speed, experienced by the kite is a combination of true wind and the kite's own flying speed. (For the time being the forward speed of the ship which also provides a wind component entering the FE is not explicitly considered. It is introduced later on.)

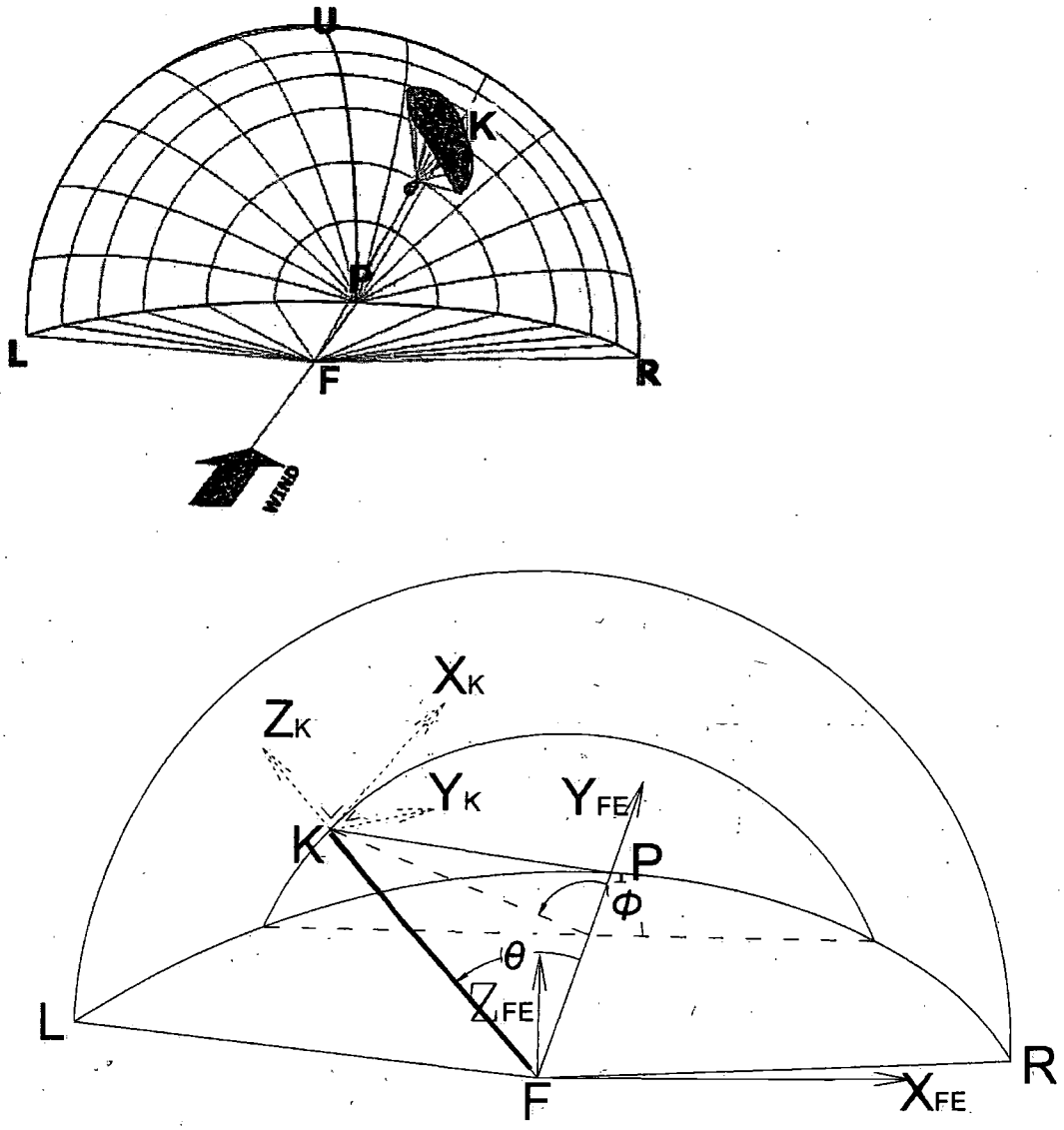

Fig. 2. Flight envelope (FE).

Depending on the position, the kite will develop its flying speed in such a way that the resulting force is parallel to the tow line. It's the main purpose of the kite performance calculation to determine this equilibrium speed and the resulting towing force.

2.2. *Flight envelope*

The set of possible positions in space of a kite, attached to a tow line with length r, is described by a quarter sphere with radius r, which is called the flight envelope (FE). See Fig. 2 where the direction of the true wind is indicated. True wind speed is defined by W. Point F is the attachment point of the tow line. The half circle

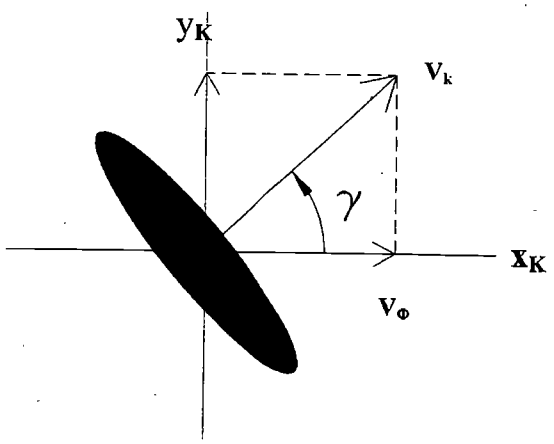

Fig. 3. Kite in projected plane of FE.

LUR is called the edge of the FE. P is the centre of the so-called power zone. When assuming uniform inflow over the altitude in the FE, P is the point where the highest speed and traction of the kite are obtained. (The effect of a boundary layer for the wind speed in which wind speed increases with altitude is discussed later on.) All half circles parallel to *LUR* are called iso-power lines: kite speed and traction are constant on these lines. All circle segments from P to the edge are iso-gradient lines: the gradient of speed and power has a constant maximum value on these lines.

The position of the kite within the FE, indicated by K is described by two angles (see Fig. 2):

- θ is the inclination of the tow line FK with respect to the line FP;
- Φ is the inclination of the plane $FK\bar{P}$ with respect to the horizontal plane.

In order to describe the flying direction of the kite, a kite reference system x_K, y_K, z_K is defined having its origin at K. The x_K axis is tangential to the iso-power line through K pointing from L to R, while the y_K axis is tangential to the iso-gradient line through K pointing towards P. The z_K axis is parallel to the tow line, pointing out of the FE.

γ is the angle between the flying direction of the kite and the positive x_K axis. See Figure 3 showing a top view (looking in negative z_K direction) on the kite.

Having defined how the kite's position and flying direction are described, this definition is used now to formulate the apparent wind experienced by the kite.

First, the apparent wind is split up into a part tangential to the FE (v_t) which is a combination of tangential velocities v_{t-x} and v_{t-y} in x_K and y_K direction respectively, and a radial part parallel to the tow line in the z_K direction (v_{r-z}).

The tangential velocity is caused by a combination of true wind and kite speed. The part due to the kite speed can be split up into a part tangential to the iso-power lines in the direction of x_K (v_{x-k}) and a part tangential to the iso-gradient lines in the direction of y_K (v_{y-k}). In y_K direction, there is a contribution by the true wind

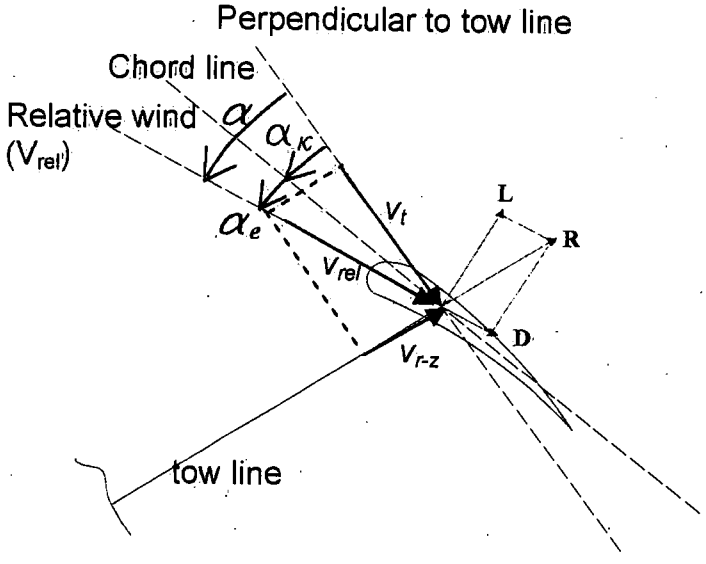

Fig. 4. Kite angle of attack.

(v_{y-w}) as well. With the above mentioned definitions, the following formulae for these velocities can be found:

$$v_{t-y} = -r\dot{\theta} + W\sin(\theta) = v_{y-k} + v_{y-w}, \tag{1}$$

$$v_{t-x} = -r\sin(\theta)\cdot\dot{\phi} = v_{x-k}. \tag{2}$$

Combining these two contributions to the total tangential velocity yields:

$$v_t = \sqrt{(v_{t-x})^2 + (v_{t-y})^2}. \tag{3}$$

For the flying speed v_k and direction γ of the kite follows:

$$v_k = \sqrt{v_{y-k}^2 + v_{x-k}^2}, \tag{4}$$

$$\gamma = \arctan\left(\frac{v_{y-k}}{v_{x-k}}\right). \tag{5}$$

The radial velocity is caused by true wind only:

$$v_{r-z} = W\cos(\theta). \tag{6}$$

With the above defined velocities, a formula for the total relative velocity v_{rel} and the angle of attack α experienced by the kite can be derived: (See Fig. 4 which depicts a cross section of the kite and the involved angle of attack.)

$$v_{\text{rel}} = \sqrt{(v_t)^2 + (v_{r-z})^2}, \tag{7}$$

$$\alpha = \arctan\left(\frac{v_{r-z}}{v_t}\right). \tag{8}$$

To find the *effective* angle of attack, α_e, the angle at which the kite is attached to the tow line, α_k, has to be subtracted from α. (Fig. 4)

$$\alpha_e = \alpha - \alpha_k. \tag{9}$$

2.3. *Lift and drag*

To determine the resulting force on the kite, first lift and drag of the 2D airfoil are determined. Corrections to these 2D lift and drag coefficients are made in order to take into account 3D induced drag and the curvature of the kite. Furthermore some additional contributions to the drag are considered which take into account line drag, inlet drag, and drag due to irregularities and surface roughness.

2D lift and drag coefficients are calculated by the free available panel method program XFOIL by Drela and Youngren [1]. The inviscid flow calculated by the program is constructed by a superposition of three potential flows being the free stream, a flow created by a vortex sheet on the airfoil surface and a source sheet on the airfoil surface and wake.

The viscous part of the solution resulting in frictional resistance is described by boundary layer shape parameter equations. For a detailed description of XFOIL reference is made to Drela and Youngren [1].

Calculation of the viscous drag requires the value of the Reynolds number which in its turn depends on the total velocity experienced by the kite, v_{rel}. However, it is v_{rel} that has to be solved by the kite performance calculation and therefore is not known at the moment lift and drag are calculated. This would require an iterative calculation procedure. However, for the Reynolds regime the kite will be operating in, the 2D drag coefficient will not vary much with the Reynolds number. Therefore, in order to avoid a time consuming iterative process, a reference velocity equal to the mean calculated v_{ref} is chosen, based on which the Reynolds number is calculated.

For more detailed information about the calculation of 2D lift and drag coefficients, reference is made to Drela [2].

The obtained 2D lift and drag coefficients have to be corrected in order to include 3D effects. This is done based on Prandtl's lifting line theory assuming elliptical lift distribution over the wing span. According to this theory, 3D effects cause an increase of the drag coefficient and a decrease of the lift coefficient:

$$C_D = c_d + \frac{C_L^2}{\pi AR}, \tag{10}$$

where:

C_D = 3D drag coefficient;

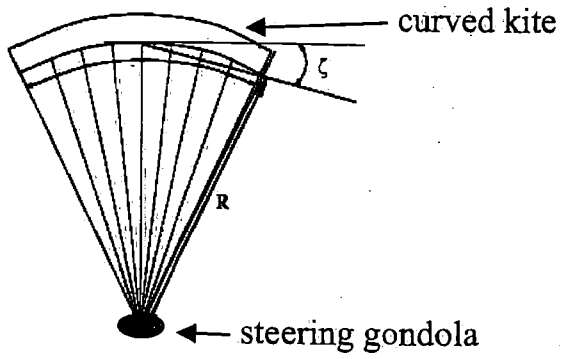

Fig. 5. Lines between gondola and kite.

c_d = 2D drag coefficient;
C_L = 3D lift coefficient;
AR = Aspect Ratio.

$$C_L = \frac{a_0}{1 + a_0/\pi AR}(\alpha - \alpha_{L=0}), \tag{11}$$

where:

C_L = 3D lift coefficient;
a_0 = 2D lift slope (which follows from 2D XFOIL calculations);
α = angle of attack;
$\alpha_{L=0}$ = zero lift angle of attack (zero for symmetric foil shapes);
AR = Aspect Ratio.

The fact that a kite has a certain span wise curvature will also result in a decrease of lift (see Fig. 5). According to Lingard [4], this effect can be formulated as follows:

$$C_{L,c} = C_L \cos^2(\zeta), \tag{12}$$

where:

C_L = 3D Lift coefficient of straight wing;
$C_{L,c}$ = 3D Lift coefficient of curved wing;
ζ = angle of curvature (see Fig. 5.)

For determining the line drag the part of the tow line underneath the gondola and the part between gondola and kite are considered separately. For the lower part it appeared that even when taking into account a line drag coefficient of 3, the drag of the tow line did not exceed 1% of the total drag (partly because the speed of the tow line itself is low). Therefore the lower tow line drag is neglected. (It must be noted however that an increase in line drag can be expected due to vortex induced vibrations which is not taken into account here.) The lines between steering gondola and kite, where the speed is assumed to equal the speed of the kite itself, appear

to generate a considerable amount of drag. The drag coefficient of all these lines together can be determined using the formulation of Prakash [5]:

$$C_{D,l} = \frac{n \cdot R \cdot d \cos^3(\alpha_l)}{S}, \tag{13}$$

where:

$C_{D,l}$ = drag coefficients of lines between gondola and kite;
n = number of lines;
R = length of lines between gondola and kite;
d = diameter of individual lines;
α_l = angle of attack between relative speed and kite line;
S = kite area.

According to Prakash [5] the number of lines depends on the kite aspect ratio as follows:

$$n = 8 + 16AR. \tag{14}$$

The diameter of the individual lines between gondola and kite is chosen such that their total cross sectional area equals that of the tow line between gondola and ship.

Other additional drag coefficients come from the air inlet, and surface irregularities and surface roughness. The air inlet is an opening at the nose of the kite enabling air flow into the inflatable kite. Prakash [5] gives approximations for drag coefficients of these components:

$$C^s_{D_{ZL}} = 0.004, \tag{15}$$

where:

$C^s_{D_{ZL}}$ = zero lift surface irregularities and fabric roughness drag coefficient.

$$C^n_{D_{ZL}} = 0.5h/c, \tag{16}$$

where:

$C^n_{D_{ZL}}$ = zero lift inlet drag coefficient (due to open airfoil nose);
h = height of the inlet (following Prakash [5] h equals $0.14*c$ for the considered kite);
c = cord length of the wing profile.

2.4. Equilibrium kite velocity

As mentioned, the key assumption of the presented approach to calculate the kite traction is the resultant force on the kite being parallel to the tow line. When assuming that the Reynolds number (based on which the 2D lift and drag coefficients are calculated) is independent of the instantaneous relative kite velocity v_{rel} and as a consequence independent of the position of the kite in the FE, the Lift to Drag ratio (L/D) is also independent of the kite position. This means that the direction of the resultant kite force depends on the angle of attack only. With a known L/D, the required angle of attack for which the resultant kite force is parallel to the tow line is easily determined and also independent of the kite position. Equation (8) gives the relation between angle of attack and radial and tangential relative velocity of the kite. The radial velocity v_{r-z} is a result of true wind only (equation (6)) and depends on the position of the kite on the FE. The tangential velocities v_{t-y} and v_{t-x} however are strongly dependent of the kite's own speed in terms of $\dot{\phi}$ and $\dot{\theta}$. So for a given flying direction γ and a given position on the FE (defined by and ϕ and θ), the required angle of attack for which the resultant force on the kite is indeed parallel to the tow line can be obtained by tuning the kite's own speed in terms of $\dot{\phi}$ and $\dot{\theta}$:

By combining equations (1), (2) and (5) $\dot{\theta}$ can be expressed as follows:

$$\dot{\theta} = -\sin(\theta) \cdot \dot{\phi} \tan(\gamma). \tag{17}$$

By substituting equation (17) and equations (1) and (2) in the expression for the angle of attack (8), a quadratic equation for ϕ can be obtained:

$$\dot{\phi}^2(r^2 \sin^2(\theta) \cdot (1 + \tan^2(\gamma))) + \dot{\phi}(2r \sin(\theta) \tan(\gamma)) = -W^2 \sin^2(\theta) + \left(\frac{W \cos(\theta)}{\tan(\alpha)}\right)^2. \tag{18}$$

Having solved $\dot{\phi}$ from equation (18), $\dot{\theta}$ follows from equation (17).

Knowing the kite velocities the instantaneous relative velocity v_{rel} of the kite is known which enables the calculation of the resultant force on the kite from the lift and drag force:

$$L = 1/2 \rho v_{\text{rel}}^2 S \cdot C_L, \tag{19}$$

$$D = 1/2 \rho v_{\text{rel}}^2 S \cdot C_D. \tag{20}$$

As mentioned calculation of lift and drag coefficients is based on a constant Reynolds number (independent of location in the FE and) independent of the instantaneous relative velocity of the kite. Therefore the lift to drag ratio is also independent of the location on the FE and only depending on the angle of attack. The angle α_k between

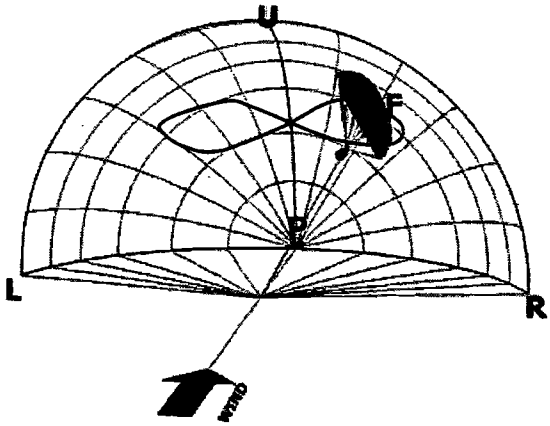

Fig. 6. Kite orbit on FE.

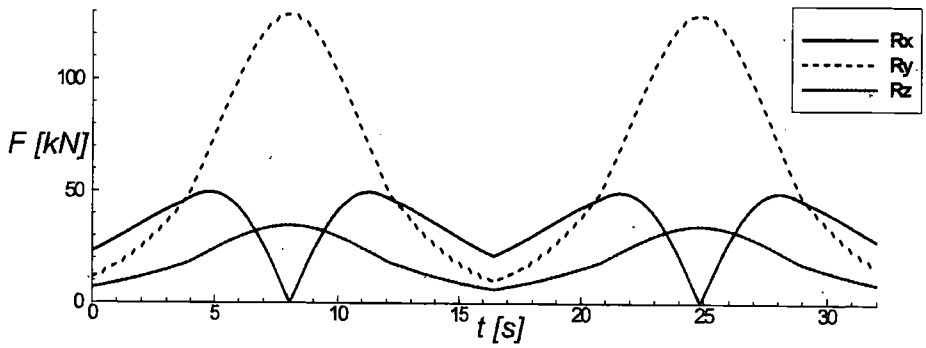

Fig. 7. Time traces of kite forces during one revolution over the orbit.

kite cord line and tow line has been chosen such that the angle of attack for which the resultant force is parallel to the tow line is giving the maximum lift to drag ratio. For the kite considered during the case study that will be described in the last paragraph, this L to D ratio amounts to 3.5.

2.5. *The flight envelope on the ship*

As mentioned, one of the benefits of a kite is that its relative velocity can be increased by actively maneuvering it on a desired track on the FE.

Such a track could be an orbit shaped as depicted in Fig. 6.

When a certain track is prescribed, total relative kite velocity and traction force at a number of points on the track can be determined. The average traction force and its direction can be calculated by a time integration over the chosen orbit. In the present study an orbital shape as depicted in Fig. 6 is considered.

Figure 7 shows a typical result for time traces of the kite forces in the FE system of axes (X_{FE}, Y_{FE}, Z_{FE}, as indicated in Fig. 2). Towing line length and wind speed amount to 150 m and 12.6 m/s respectively. At an average flying altitude of 30% of the towing line length the wind speed amounts to 14.6 m/s. This example concerns

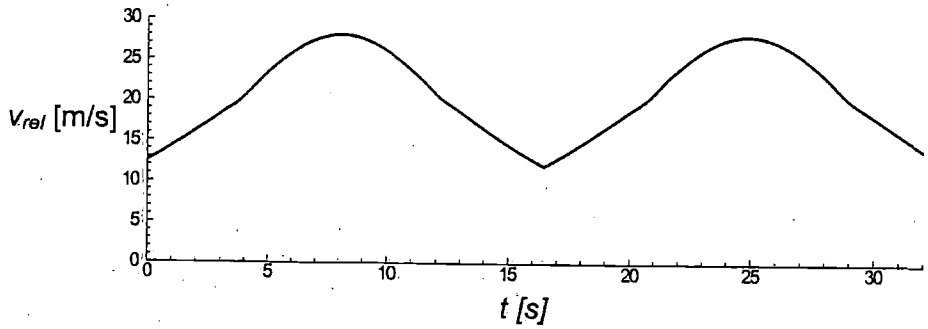

Fig. 8. Time trace of relative velocity experienced by the kite.

a ship sailing at 15.5 kn with wind from the stern (resulting in a netto wind speed of 6.6 m/s entering the FE at average kite altitude). The area of the kite is 500 m^2. Starting a small distance off the edge of the FE at $t = 0$ s, the kite flies in the direction of the power zone at almost constant altitude. The y-force increases, reaching a maximum when the kite crosses the Y_{FE}-axis. The other edge is reached at approximately $t = 16$ s after which the kite flies back to the edge where the orbit was started.

The velocity v_{rel} along the track for the same conditions is shown in Fig. 8.

When the kite passes through the power zone relative velocities of up to 28 m/s occur being 4.2 times the netto wind speed entering the FE at kite altitude.

In case of a kite towing a ship, the wind that enters the FE (being called 'true' wind until now) is in fact a combination of true wind and wind created by the ship's own speed. In general the direction of these two will not coincide. The FE is positioned on the ship in such a way that its edge is perpendicular to the direction of combined true wind and ship speed. However, true wind varies with altitude and as a consequence, direction of combined true wind and ship speed varies with altitude as well. That is why for determining the direction of the FE, true wind at a reference height equal to the average flying altitude of the kite's orbital track is used. As the kite's flying altitude is supposed to be within the so-called surface layer of the atmosphere, where the occurring wind is dominated by pressure differences and no geotropic winds occur, the variation of wind speed with altitude can be expressed by a logarithmic profile (Troen [3]):

$$W(z) = C_{\log} \ln\left(\frac{z}{z_0}\right), \tag{21}$$

where:

$W(z)$ = Wind speed at altitude z above (sea) surface.

$$C_{\log} = \frac{u_{\text{ref}}}{\ln(z_{\text{ref}}/z_0)},$$

where:

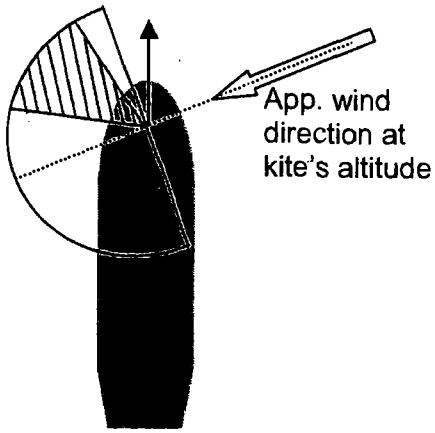

Fig. 9. Top view FE on ship.

u_{ref} = known wind speed at reference level;
z_{ref} = reference level (10 m);
z_0 = surface roughness (depending on wave height).

Figure 9 depicts a top view on ship and FE. Depending on the direction of the apparent wind with respect to the sailing direction, a certain range of horizontal kite positions can be defined resulting in a traction force having a component in the ship's sailing direction. Taking into account the fact that the practical boundaries of the 'accessible area' of the kite are a bit off the edge of the FE, this range is indicated by the hatched area in Fig. 9.

Concerning the vertical position of the kite orbit, an optimum can be found resulting in the highest mean traction force in the ship's sailing direction.

This optimum flying altitude is governed by:

the variation of traction force over the FE;
the variation of wind velocity over altitude;
variation of horizontal component of traction force with varying angle between tow line and horizontal plane.

To assess the effect of the flying altitude on the kite force in the direction of the forward speed X_{kite}, and to find the optimum flying altitude in terms of maximum X_{kite}, simulations of the kite, flying along an orbital track, have been made for various flying altitudes during a case study. Details about the case study are presented in the last paragraph. For three different towing line lengths, 150 m, 350 m and 550 m and three different wind speeds, the traction force in the direction of the forward ship speed (time-averaged over one revolution on the orbit) has been calculated for various flying altitudes. Results for a towing line length of 150 m are presented in Fig. 10.

It appears that the altitude at which maximum forward towing force occurs amounts to 27 to 33% of the towing line length, slightly decreasing with increasing wind speed.

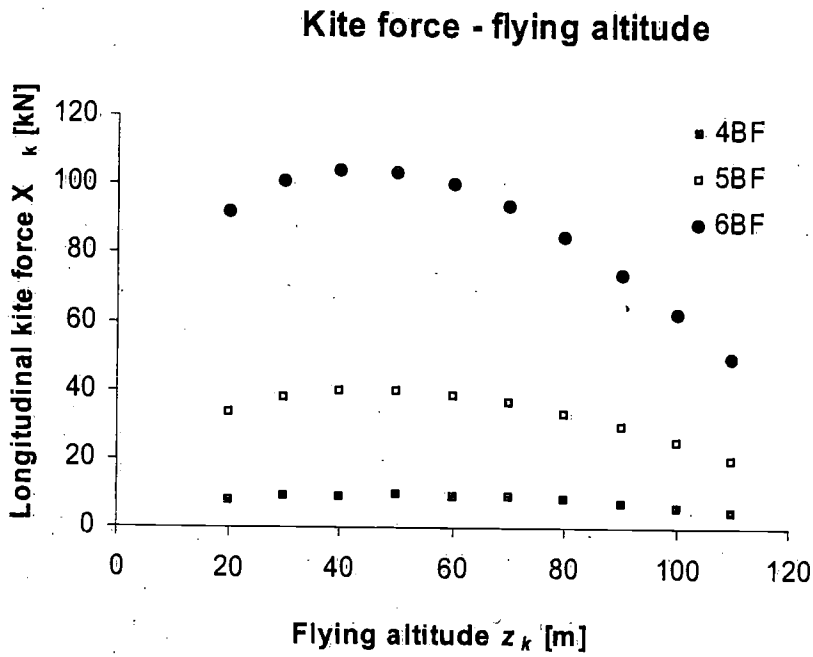

Fig. 10. Kite force as a function of flying altitude for line length = 150 m.

Above presented results are for a wind direction of 0 degrees off the stern. Similar calculations have been made for different wind directions resulting in optimum flying altitudes in the same range.

3. Performance prediction

3.1. Introduction

Having determined the forces on the kite, these are now considered as external forces acting on the ship. The presence of this external force effects the fuel consumption of the ship. Basically there are two effects that will be addressed:

1. Besides a kite force component in the direction of the forward speed, there will in general also be a component perpendicular to this, resulting in a side force and yawing moment. The resulting drift angle of the ship and rudder angle needed to ensure lateral force balance and yaw balance will effect the resistance of the ship.
2. Due to the thrust provided by the kite, the existing propulsion installation will be operated at off-design situations. The performance of propeller and main engine in combination with a kite will be considered in order to determine the fuel consumption.

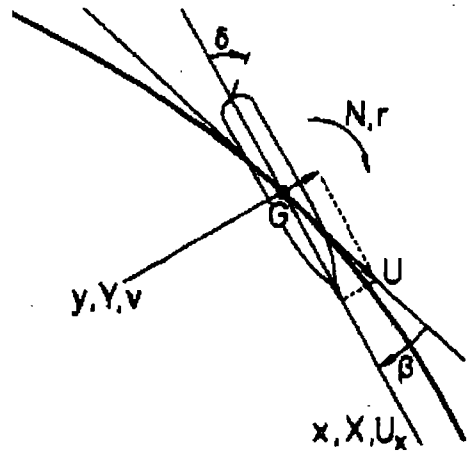

Fig. 11. Hydromechanic forces on ship's hull.

3.2. *Hull hydromechanics*

Figure 11 defines the involved forces, moments, velocities and angles involved in case of a partly kite-propelled ship sailing with a certain steady drift angle β.

Writing the hydromechanic hull and rudder forces and moments in terms of the usual maneuvering coefficients neglecting third and higher order terms, the following formulations yield for the horizontal force and moment balance:

lateral force balance:

$$Y_{\text{kite}} + Y_v v + Y_\delta \delta + Y_{\delta\delta}\delta^2 = 0, \tag{22}$$

longitudinal force balance:

$$\begin{aligned} &X_{\text{kite}} + X_{\text{prop}} - R + X_{vv}v^2 + X_{\delta\delta}\delta^2 + X_{v\delta}v\delta \\ &\quad = X_{\text{kite}} + X_{\text{prop}} - R + X_{\text{i}} = 0, \end{aligned} \tag{23}$$

yaw balance:

$$N_v v + N_\delta \delta + N_{\delta\delta}\delta^2 + Y_{\text{kite}} \cdot x_{\text{kite}} = 0, \tag{24}$$

where:

v = lateral ship speed;
δ = rudder angle;
subscripts v and δ denote derivatives to lateral speed and rudder angle;
Y, X, and N = lateral force, longitudinal force and yaw moment where subscript *kite* denotes forces induced by the kite;
X_{i} = induced longitudinal force due to rudder angle and drift: $X_i = X_{vv}v^2 + X_{\delta\delta}\delta^2 + X_{v\delta}v\delta$;

X_{prop} = longitudinal force provided by propeller;
R = calm water ship resistance;
x_{kite} = distance between kite attachment point and ship's centre of rotation (COG).

From the equations for the lateral force balance and yaw balance, v and δ can be found by simultaneously solving these equations. Knowing these, the required propeller force X_{prop} can be found from the longitudinal force balance. However, rudder force coefficients N_δ and $N_{\delta\delta}$ are dependent of the flow velocity at the rudder which in its turn depends on the increase of flow velocity due to the propeller. The latter is governed by the thrust that has to be delivered by the propeller and therefore there is a coupling between the equation for the longitudinal force balance (23) and those for the lateral force and horizontal moment balance, (22) and (24). The effect of the lateral ship speed, v, on the propeller performance (among others the propeller producing a side force in an inclined incoming flow) has been ignored.

Obviously the hydromechanic yaw moment on the hull ($N_v v$) and the yaw moment induced by the kite ($Y_{\text{kite}} \cdot x_{\text{kite}}$) have opposite directions. The difference will have to be compensated by the rudder which will also result in extra resistance. During the case study described in the last paragraph it appeared that the optimal position of the kite attachment point (for which a minimum rudder angle is required to ensure yaw balance) is as far forward on the bow as possible.

3.3. *Engine and propeller performance*

As a result of the additional towing force by the kite, less thrust is required from the propeller. Assuming that the ship's forward speed is kept constant, a formulation is given here for determining the propeller loading and corresponding engine power and fuel consumption for this off-design condition.

The force required from the propeller follows from the longitudinal force balance (equation (23)):

$$X_{\text{prop}} = R - X_{\text{kite}} - X_{\text{i}}. \tag{25}$$

Following Kleinwoud and Stapersma [6] for one specific forward speed U, X_{prop} can be written as:

$$X_{\text{prop}} = c_1 \cdot U^2, \tag{26}$$

where c_1 is a speed dependent factor: $c_1 = (R - X_{\text{kite}} - X_{\text{i}})/U^2$.

Using the wake fraction this becomes:

$$X_{\text{prop}} = c_1 \cdot \left(\frac{v_A}{1-w}\right)^2, \tag{27}$$

where:

v_A = advance velocity at the propeller;
w = wake factor.

Taking into account thrust deduction, the required propeller thrust is equal to:

$$T_{\text{prop}} = \frac{X_{\text{prop}}}{(1-t)} = \frac{c_1 \cdot v_A^2}{(1-t)\cdot(1-w)^2} = c_8 \cdot v_A^2, \tag{28}$$

where:

t = thrust deduction fraction;
$c_8 = \frac{c_1}{(1-t)\cdot(1-w)^2}$.

For the non-dimensional thrust coefficient follows:

$$K_{T_{\text{prop}}} = \frac{c_8 \cdot v_A^2}{\rho n^2 D^4} = \frac{c_8}{\rho D^2} \cdot J^2, \tag{29}$$

where:

ρ = density of water;
n = number of propeller revolutions per second;
D = propeller diameter;
J = advance ratio: $J = v_A/nD$.

So the non-dimensional thrust has been expressed by a quadratic function of the advance ratio J. Using the propeller open water diagram J can be solved by matching the propeller's open water K_T value and the above deduced $K_{T_{\text{prop}}}$.

The corresponding torque coefficient is found from the open water K_Q curve.

Taking into account the relative rotative efficiency η_R and the transmission efficiency η_{TRM} finally the engine brake power can be found:

$$P_B = \frac{2\pi}{\eta_R \cdot \eta_{\text{TRM}}} \cdot K_Q \cdot n^3. \tag{30}$$

The fuel consumption follows from the brake specific fuel consumption *BSFC* (which is given for the considered engine) and the required brake power.

4. Case study

The theory described so far is applied to a case study. The main objective is to calculate relative fuel consumption for one specific ship, equipped with a kite of a certain size and shape for a range of environmental conditions (wind speed and wind direction). Kite forces and therefore fuel consumption strongly depend on the length of the towing line which is why the results will be presented for different towing line lengths.

Table 1
Case ship data

L_{wl}	Length water line	225.86	m
L_{oa}	Length over all	231.34	m
B	Beam	29.57	m
D	Draught	12.5	m
Δ	Displacement	66716.225	t
Vs	Ship service speed	15.5	kn
A_T	Transverse projected area ship above water	430	m^2
A_L	Lateral projected area ship above water	1810	m^2
X_z	Fixation point kite measured from the centre of rotation	100	m
S_h	Wetted area	10108	m^2
n_p	Revolutions per minute of the propeller {design + sea margin}	107	rpm
n_p	Revolutions per minute of the propeller {design}	100	rpm
P_b	Brake power of the engine {design}	12000	kW
BSFC	Brake specific fuel consumption: $BSFC = 43.53(P^*)^2 - 78.111(P^*) + 196.8$		g/kWh
D_p	Propeller diameter	6.706	M
T	Thrust deduction factor	0.187	–
W	Wake factor	0.324	–
k_p	Number of propellers	1	–
C_t	Total resistance coefficient	0.002414	–
η_r	Relative rotative efficiency	0.99	–
η_{tr}	Transmission efficiency	0.97	–

4.1. Case ship

To carry out this study, the 50.000 dwt tanker 'British Bombardier' served as a case ship. One reason for choosing this rather old tanker is that a slow ship (the service speed of the British Bombardier is 15,5 kn) is likely to benefit the most from wind propulsion as the apparent wind direction will be relatively more from the stern than will be the case for a faster ship type. Another reason is that extensive model experiments have been carried out by Journee [7] at the Delft University Ship Hydromechanics Laboratory in the late 60's with a model of this particular ship providing all the necessary hydromechanic data on the hull to perform the performance prediction calculations. The ship was originally equipped with a steam turbine. For this study an equivalent diesel engine was considered. In Table 1 the main particulars and all quantities relevant to the performance prediction of the case ship are summarized.

The brake specific fuel consumption in g/kWh (BSFC) is given as a quadratic function of the normalized brake power P^* (which is a fraction of the nominal power).

The non-dimensional hydromechanic maneuvering coefficients were taken from Journee [7]. Forces and moments were normalized by dividing by $0.5\rho U^2 L^2$ and

Table 2
Hydromechanic coefficients case ship

Y'_{δ}	Dimensionless force due to δ in Y direction	3.13E-03	[–]
$Y'_{\delta\delta}$	Dimensionless force due to δ^2 in Y direction	3.79E-04	[–]
Y'_{v}	Dimensionless force due to v in Y direction	−1.80E-02	[–]
N'_{v}	Dimensionless moment due to v in Z direction	−4.73E-03	[–]
N'_{δ}	Dimensionless moment due to δ in Z direction	−1.55E-03	[–]
$N'_{\delta\delta}$	Dimensionless moment due to δ^2 in Z direction	−1.13E-04	[–]
$X'_{v\delta}$	Dimensionless force due to v$*\delta$ in X direction	1.17E-03	[–]
X'_{vv}	Dimensionless force due to v^2 in X direction	9.40E-04	[–]
$X'_{\delta\delta}$	Dimensionless force due to δ^2 in X direction	−1.62E-03	[–]

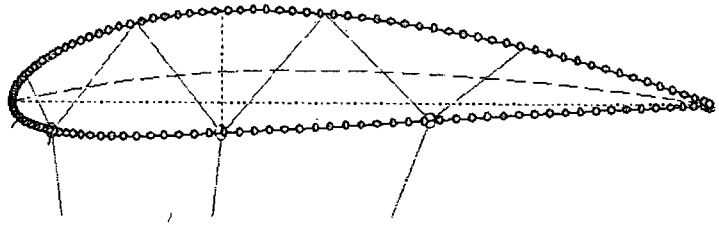

Fig. 12. Cross sectional shape of kite: NACA 4415.

by $0.5\rho U^2 L^3$ respectively (where U is forward speed and L is ship length). The coefficients are derivatives of the normalized forces and moments to the concerning dimensionless quantities. (So e.g. Y'_v has to be multiplied by v/U (the dimensionless drift velocity) to obtain the dimensionless Y-force.) The hydromechanic coefficients are listed in Table 2.

4.2. Case kite

For the cross sectional shape a similar airfoil shape was used as is often applied for kite surfing which is a NACA 4415, depicted in Fig. 12. A wing with an area of 500 m^2 and an aspect ratio of 4 was adopted having an elliptical cord length distribution over the span.

4.3. Results and discussion

The theoretical fuel saving that can be achieved in the considered case is presented by the polar diagram in Fig. 14 for a towing line length of 150 m. The angular axis represents the true wind direction from the bow. The radial distance from the origin represents the fuel consumption as a percentage of the fuel consumption as it would be without using the kite. The different lines represent different wind speeds as indicated in the legend. In all calculated conditions wind resistance and added resistance in waves is included. (Wind resistance is calculated according to Isherwood [8]. For added resistance in waves model test results have been used [7].)

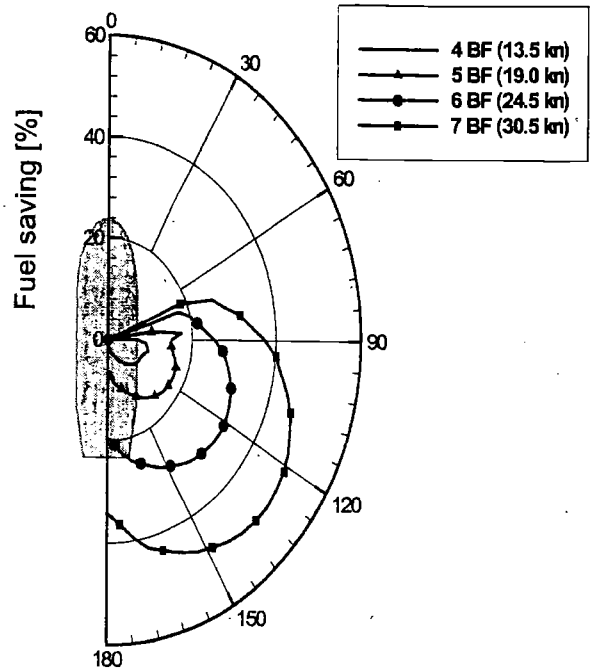

Fig. 13. Relative fuel saving, 350 m line length.

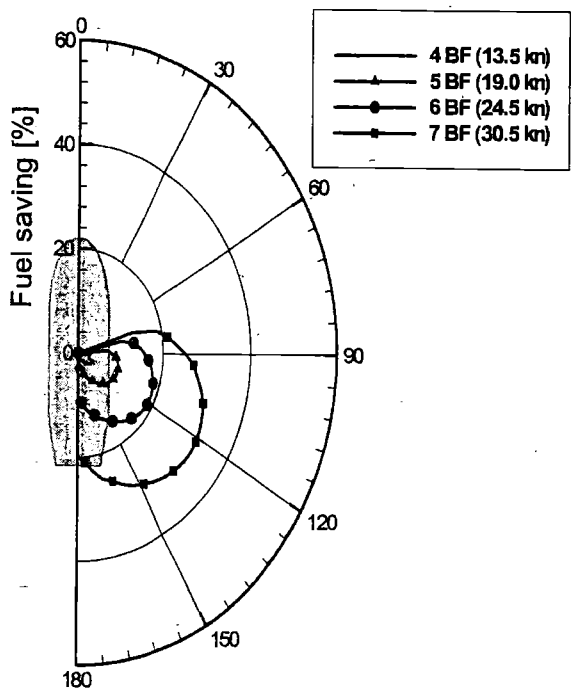

Fig. 14. Relative fuel saving, 150 line length.

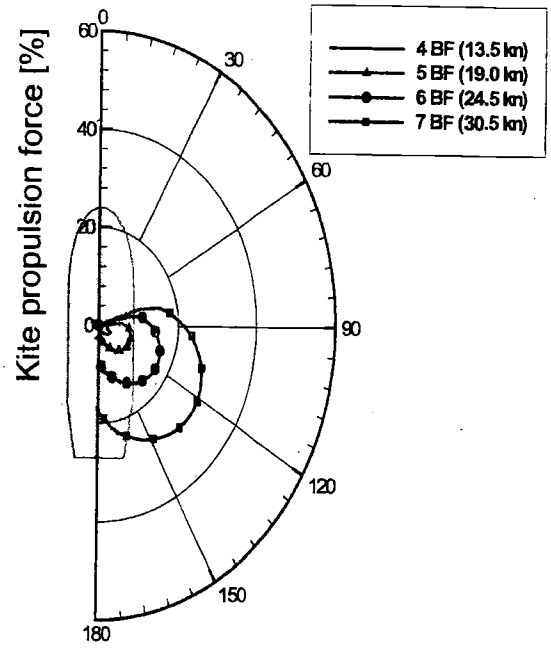

Fig. 15. Relative propulsion force by kite.

For upwind conditions, the kite cannot be operated as the apparent wind direction simply leaves no accessible area where the kite is able to fly a prescribed orbit resulting in a propulsive force (see Fig. 9). This is why no fuel saving is obtained for upwind true wind directions.

As can be seen, fuel saving rapidly increases with wind speed. For a wind speed of 6 Beaufort and a towing line length of 150 m fuel saving amounts to 19% at the most favorable wind direction which is approximately 120 deg off the bow. A towing line length of 350 m (see Fig. 13) results in 33% fuel saving for the same condition. For 7 Beaufort the saving percentages amount to 35% and 50% for the mentioned towing line lengths respectively.

Figure 15 shows the force delivered by the kite in the direction of the forward speed as a percentage of the total resistance without kite for a towing line length of 150 m. One would expect this percentage to be higher than the relative fuel saving: drift induced resistance and unfavorable off-design operation of the existing propulsion installation would result in a relative decrease of fuel consumption that is less than the relative decrease in required mechanical propulsion force (*relative* to the situation without a kite). However, this is not the case. Relative fuel saving even slightly exceeds the relative propulsion force by the kite in some cases. An explanation for this can be found in the open water propeller efficiency. See Fig. 16 which shows the open water propeller characteristics for the case ship.

The design point (without kite) and the off design condition (with kite) for maximum kite propulsion force at Beaufort 7 are indicated. The figure shows that the open water efficiency changes from 0.59 to 0.63, an increase of 6.8%. A similar effect was

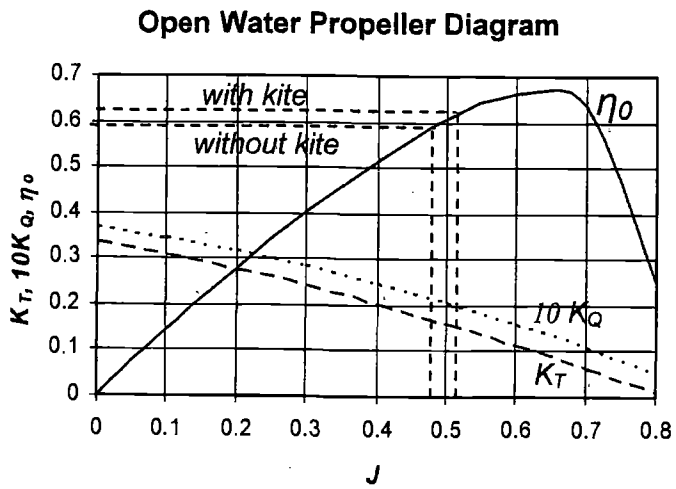

Fig. 16. Open water propeller diagram.

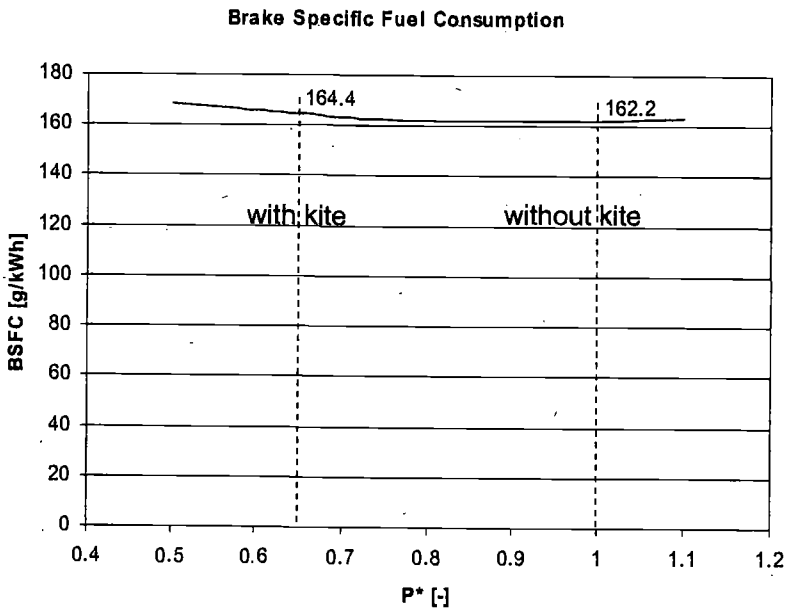

Fig. 17. Brake specific fuel consumption.

also mentioned by Molland [9]. The increase of open water efficiency appears to be much larger than the increase of brake specific fuel consumption (BSFC) for this case which is indicated in Fig. 17.

The figure shows the BSFC of the engine [g/kWh] against nomalized brake power, P^*. As can be seen the increase in BSFC due to off design operation (with kite) is not that large compared to the nominal situation (without kite): the increase amounts 1.4%.

Another expected unfavorable effect on the fuel consumption comes from the transverse force and resulting yaw moment induced by the kite. Due to this, a certain

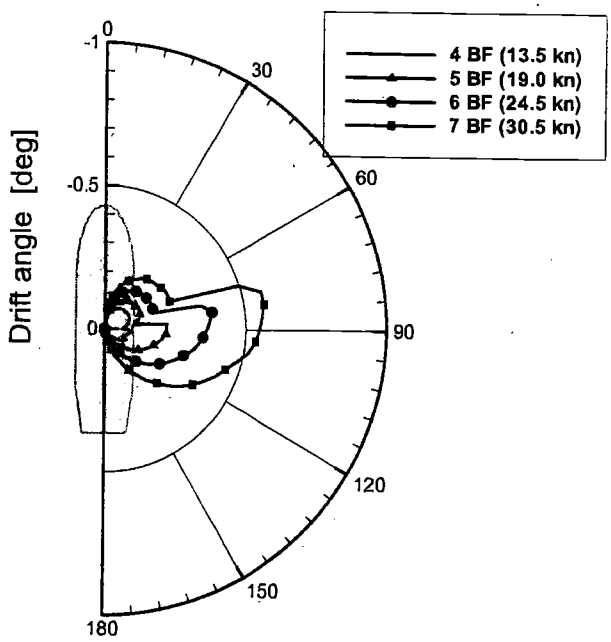

Fig. 18. Drift angle.

drift angle and rudder angle will be required to obtain force balance in transverse direction and yaw moment balance. Both will result in an increase of resistance. Figure 18 shows a polar diagram of the drift angle required to obtain transverse force balance on the hull. As can be seen the maximum drift angle that will occur amounts to 0.6 degrees.

Yaw balance is obtained by using the rudder. Rudder angles are presented in Fig. 19. The rudder moment ($N_\delta\delta + N_{\delta\delta}\delta^2$ in equation (24)) and hydrodynamic moment on the hull ($N_v v$ in equation (24)) have opposite directions. From this it can be concluded that the optimal position to attach the kite is at the bow of the ship, thus minimizing the required rudder angle to obtain yaw balance.

The total induced resistance by drift and rudder angle is presented relative to the total resistance without kite in Fig. 20. As can be seen drift and rudder induced resistance only amount to at most 0.65%.

4.4. *Economy*

It should be noted that mentioned numbers concerning fuel saving correspond to certain ideal environmental conditions: they do not conclude on long term benefits which will obviously be lower. Further research is being carried out to assess the long term benefits of auxiliary kite propulsion. Voyage simulations will be done and the effect of routing will be considered: especially when using wind propulsion, it is expected that route optimization will have a significant effect on long term fuel saving.

The actual economic performance of the system will depend on many factors. The most important ones seem:

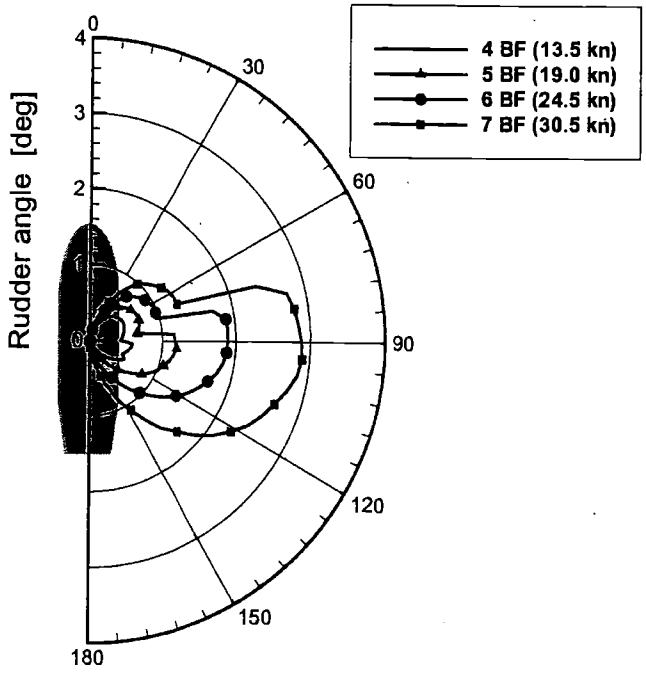

Fig. 19. Rudder angle.

- the wind and wave climate on the operational route (the frequency and persistance of favourable winds);
- the possibilities to use weather routing and the accuracy of these forecasts;
- the practical operational limits of the kite deployment.

An economic optimisation requires a tradeoff of the ships prime performance indicators which are:

- the mean trip duration;
- the irregularity of the trip duration;
- the fuel consumption.

Ways to balance the mean trip duration against fuel costs are well developed (Evans [10]). The irregularity of a ship's service, which is expected to increase with maximum use of favourable weather to save fuel, seems more difficult to assess. Scenario simulations (Dallinga [11]) that account for the masters actions to optimize the balance between fuel and arrival time and which are based on contemporary climate descriptions seem to offer a way to quantify the economics.

4.5. Conclusions and recommendations

- Theoretical fuel saving for a 50.000 dwt tanker can amount to up to 50% at Beaufort 7 with stern quartering wind using a kite of 500 m^2 attached to a 350 m towing line.

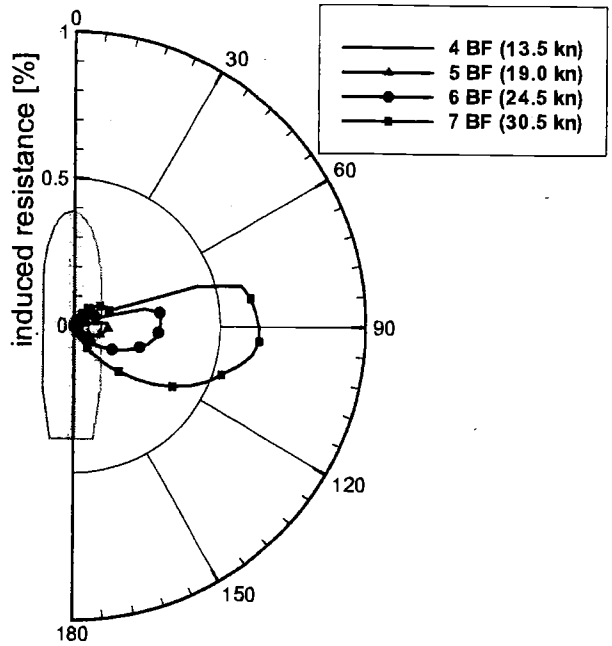

Fig. 20. Induced resistance.

- Optimal flying altitude for the considered towing line lengths (150–550 m) amounts to 30% of the towing line length.
- Attaching the towing line to the bow minimizes required rudder angles.
- Losses due to drift, rudder angle and off design operation of the engine are small and counteracted by an improved open water propeller efficiency resulting in a relative fuel saving that roughly equals the relative traction force delivered by the kite.

The major uncertainties involved in the presented analysis are introduced by the calculation of the kite force. It is not known how valid the quasi-static approach is which is another reason to interpret presented fuel saving numbers carefully. Validation of the kite force calculation is desired as well as further research to the optimization of the kite's orbit.

Future work will aim to estimate long term fuel saving for which voyage simulations including the effect of route optimization will have to be carried out.

References

[1] M. Drela and H. Youngren, *XFOIL 6.94 User Guide*, MIT Dept. of Aerodynamica and Astrodynamics, Aerocraft, Inc, 2001 (http://raphael.mit.edu/xfoil/xfoil_doc.txt).

[2] M. Drela, *An analysis and design system for low Reynold's number airfoils*, MIT Dept. of Aerodynamica and & Astrodynamics, 1989.

[3] I. Troen and E.L. Petersen, *European Wind Atlas*, Riso National Laboratory, 1989.

[4] J.S. Lingard, Ram-air Parachute Design, in: *Precision Aerial Delivery Seminar, 13th AIAA Aerodynamic Decelerator Systems Technology Conference*, Clearwater Beach, 1995.

[5] O. Prakash, *Aerodynamics and Longitudinal Stability of Parafoil/Payload System*, Department of Aerospace Engineering, Indian Institute of Technology, Bombay, 2004.

[6] H. Kleinwoud and D. Stapersma, *Design of Propulsion and Electric Power Generation Systems*, London, Imarest, 2003.

[7] J.M.J. Journee and D. Clarke, Experimental Manoeuvring Data of Tanker "British Bombardier", Report No. 1429 Delft University of Technology Ship Hydromechanics Laboratory, Delft, 2005.

[8] R.M. Isherwood, *Wind Resistance of Merchant Ships*, Trans. of the Royal Institution of Naval Architects, 1973.

[9] A.F. Molland, Operation of Propellers and Machinery in Wind Assisted Ships, in: *Proc. of the First Wind Assisted Ship Propulsion Symposium*, Glasgow, 1985.

[10] J. Evans and P. Marlowe, *Quantitative methods in Maritime Economics*, Fairplay Publications, 1990, ISBN 1870093 31 3.

[11] R.P. Dallinga, E.F.G. van Daalen, R. Grin and A.P. Willemstein, *Scenario Simulations in Design for Service*, PRADS, 2004.

International Shipbuilding Progress 53 (2006) 311–312
IOS Press

Author Index Volume 53 (2006)

The issue number is given in front of the page numbers.